J. Fluid Mech. (2013), *vol.* 721, *pp.* 324–339.
doi:10.1017/jfm.2013.69

Nonlinear analysis of shock–vortex interaction: Mach stem formation

Paul Clavin†

Aix-Marseille Université, CNRS, IRPHE, F-13013 Marseille, France

(Received 19 November 2012; revised 24 January 2013; accepted 28 January 2013;
first published online 13 March 2013)

Shock–vortex interaction is analysed for strong gaseous shock waves and a ratio of specific heats close to unity. A nonlinear wave equation for the wrinkles of the shock front is obtained for weak vortices. The solution breaks down after a finite time and the slope of the front develops jump discontinuities, indicating the formation of Mach stems. Shock–turbulence interactions are also briefly discussed.

Key words: nonlinear dynamical systems, shock waves, wave–turbulence interactions

1. Introduction

For a long time gaseous planar shock waves have been known to be stable. Experimental and theoretical pioneering studies reported a relaxation of initial disturbances which follows power laws, $t^{-1/2}$ or $t^{-3/2}$, see Lapworth (1959), Briscoe & Kovitz (1968) and Van-Moorhem & George (1975). The stroboscopic schlieren photographs, taken to study the relaxation, show Mach stems (triple points) propagating in the transverse direction on the shock front. Except for the approximate geometrical approach of Whitham (1957), no particular attention was paid to these phenomena in the past.

Cellular detonations are instructive examples of Mach stem formation in shock waves. Gaseous detonations consist of a strong inert shock followed by an exothermic reaction region. Planar gaseous detonations are known to be unstable and exhibit cellular structures with triple points propagating in the transverse direction of the shock front. Cellular detonations were observed a long time ago, see Shchelkin & Troshin (1965) and Strehlow (1979). More recently, the cellular structure has been explained by the weakly nonlinear analysis of Clavin & Denet (2002) near the instability threshold of planar detonations. According to this analysis, the main nonlinear effect is not associated with the heat release. This suggests that the formation of Mach stems results from some mechanism inherent in the dynamics of the shock front which is wrinkled by the instability due to an unsteady coupling with the heat release.

The early numerical simulations of two-dimensional shock–vortex interaction by Guichard, Vervich & Domingo (1995) and Ellzey *et al.* (1995) have shown that the front develops corners and triple points. The more recent numerical simulations of Inoue & Hattory (1999), Inoue (2000) and Zhang, Zhang & Shu (2005) focus attention

† Email address for correspondence: clavin@irphe.univ-mrs.fr

on sound generation for different strengths of rather strong vortices (turnover velocity v_1 of the order of the sound speed $\overline{a}_1$). These simulations are limited to weak shocks with a small Mach number of propagation $\overline{M}_1$, not larger than 1.3, the inner structure of the shock wave being resolved by using the Navier–Stokes equations. In contrast to these simulations, attention is focused here on strong shocks, $\overline{M}_1 \gg 1$, and weak vortices (very subsonic turnover velocity). Therefore, the distortions of the shock front are small, which is a necessary condition for a weakly nonlinear analysis. Moreover, strong shocks may be of interest in astrophysics and in fusion by inertial confinement.

Shock–turbulence interaction is a fundamental problem which has been extensively studied. Mach stems are not easy to observe on strongly unsteady shock waves, neither in numerics nor in experiments. However, sharp transitions in the slope of the front appear in the direct numerical simulation of Lele & Larsson (2009), see also Larsson & Lele (2009). Moreover, a strong bursting character of the flow of compressed gas is observed in the experiments of Agui, Briassulis & Andreopoulos (2005). An outcome of the present analysis is a simple nonlinear equation which can be used as a model for studying the two-dimensional geometry of the cusped front of a strong shock propagating in a weakly turbulent flow, see (4.19). From the theoretical side, analytical studies of shock–turbulence interaction have been carried out in the linear approximation, see Wouchuk & Huete Ruiz de Lira (2009) and the PhD thesis of Huete Ruiz de Lira (2012) where an extensive review of the literature may be found. Apparently, nonlinear analyses of shock–vortex interaction have not yet been performed.

The only existing systematic analysis of Mach stem formation is the weakly nonlinear analysis of Majda & Rosales (1983). This pioneering analysis concerns spontaneous Mach stem formation in a reacting shock front propagating in a quiescent medium. The front being considered as a hydrodynamic discontinuity without modifications of its inner structure, the instability mechanism of detonations is not fully taken into account. Another basic assumption of the analysis is that all of the eigenmodes are radiating (spontaneous sound emission). This assumption is not valid for inert shock waves propagating in a quiescent polytropic gas, see Clavin & Williams (2012). However, the acoustic waves generated in the compressed gas during the interaction of a shock wave with a non-uniform flow are systematically radiating. Therefore, it can be argued that Mach stem formation might not be much different from that described by Majda & Rosales (1983).

The purpose of the present work is not to solve analytically the shock–vortex interaction in the general case. An approximate solution for the formation of singularities of the slope of a weakly wrinkled shock front is obtained in a limiting case instead. Coupling vorticity and pressure waves makes the analysis difficult to carry out, especially for the initial-value problem of the shock–vortex interaction. Analytical results and physical insights cannot be easily obtained without further simplifications. In the distinguished limit (2.5) which is considered here, $\overline{M}_1 \gg 1$ and $(\gamma - 1) \ll 1$, see the formulation in § 2, the sound speed in the compressed gas, $\overline{a}_2$, is of the same order of magnitude as in the initial medium, $\overline{a}_2/\overline{a}_1 = O(1)$, but the flow of the compressed gas (velocity $\overline{u}_2$ relative to the shock front) is strongly subsonic, $\overline{M}_1 \equiv \overline{u}_1/\overline{a}_1 \gg 1 \Rightarrow \overline{u}_2 \ll \overline{a}_2 \ll \overline{u}_1$. Attention is focused on the interaction in two dimensions of a strong shock wave with a weak and rectilinear vortex of strength $2\pi r_0 v_1$ whose axis is parallel to the shock front, and $v_1 \ll \overline{a}_1 \ll \overline{u}_1$. At large distances from the vortex core, $r \gg r_0$, the small turnover velocities in the irrotational region should not play significant roles. The analysis is performed for a vortex of finite size l, and the extension to usual rectilinear vortices is discussed in § 3.7.

The physical insights may be summarized as follows. A small distortion of the shock front is formed during the short lapse of time taken by the vortex to cross the shock, $\tau_{int} = l/\overline{u}_1$, called the interaction time in the following. The amplitude of the wrinkle is much smaller than its transverse extension l, the slope of the wrinkle being of order $\overline{a}_2 v_1/\overline{u}_1^2 \ll 1$. The calculation is carried out in § 3.3 and the results are summarized in § 3.4. After the interaction time, $t > \tau_{int}$, the wrinkled shock wave propagates into a quiescent medium, as is the case for the normal modes analysis. The wrinkles of the front then propagate in transverse directions at the sound velocity of the shocked gas, $\overline{a}_2$, see § 3.5. This transverse propagation involves a characteristic time longer than the interaction time, $l/\overline{a}_2 \gg \tau_{int}$. Owing to this difference of time scales, the initial condition for the second stage ($t > \tau_{int}$) is, roughly speaking, provided by the vortex–shock cross-over (first stage, $0 < t < \tau_{int}$). The analysis is simplified by the approximation in (3.14): in the limit (2.5) the flow of the impulsive source which generates an acoustic pulse during the cross-over, has a negligible transverse component. Therefore, during the second stage, the downstream compressible flow is negligibly near the shock front and the dynamics of the wrinkles is mainly controlled by an incompressible shear flow (vorticity wave), see § 3.5. Thus, the linear dynamics for $t > \tau_{int}$ is described by the wave equation (3.9) of the normal mode analysis in the limit (2.5). A composite equation, covering both the first and the second stage, is then obtained, see (3.29). The weakly nonlinear analysis is performed in §§ 4.1 and 4.2. This leads to the same nonlinear equation (4.17) as for the normal modes but with an additional impulsive source term, see (4.19). As in the works of Whitham (1957) and Majda & Rosales (1983), the solution breaks down in finite time and the slope of the shock front develops jump discontinuities, indicating the formation of Mach stems after the cross-over, and away from the impact region. The extension to three dimensions is straightforward, see (4.19). Such analytical results are obtained for weak vortices $v_1 \ll \overline{a}_1$ and strong shocks in the limit (2.5). In contrast, large distortions of the shock front and triple points are produced during the cross-over of strong vortices and weak shocks. This case is not covered by the weakly nonlinear analysis performed here. Discussion of the results, concluding remarks and perspectives are given in § 5.

2. Formulation

The shock wave is considered as a discontinuity separating two flows of a polytropic gas. The two-dimensional Euler equations may be written as

$$\frac{1}{\rho}\frac{\mathrm{D}}{\mathrm{D}t}\rho + \frac{\partial}{\partial x}u + \frac{\partial}{\partial y}w = 0, \quad \rho\frac{\mathrm{D}}{\mathrm{D}t}u = -\frac{\partial}{\partial x}p, \quad \rho\frac{\mathrm{D}}{\mathrm{D}t}w = -\frac{\partial}{\partial y}p, \quad \frac{\mathrm{D}}{\mathrm{D}t}s(\rho, p) = 0, \tag{2.1}$$

where ρ, p, s, u and w are the density, the pressure, the entropy, the longitudinal and transverse velocity of the flow, and where the material derivative has been introduced $\mathrm{D}/\mathrm{D}t \equiv \partial/\partial t + u\partial/\partial x + w\partial/\partial y$. The conditions upstream and downstream from the shock front will be identified by the subscripts 1 and 2, respectively. Introducing the ratio of specific heats γ, the jumps of ρ and p across the shock are (Rankine–Hugoniot conditions)

$$\rho_{1f}/\rho_{2f} = [(\gamma-1)M_1^2 + 2]/[(\gamma+1)M_1^2], \quad p_{2f}/p_{1f} = [2\gamma M_1^2 - (\gamma-1)]/(\gamma+1) \tag{2.2}$$

where the subscript f denotes values at the shock front. The Mach number M_1 is expressed in terms of both the upstream flow and the equation of the shock

front $x = \alpha(y, t)$,

$$M_1 = \frac{(u_{1f} - \dot{\alpha}_t - w_{1f}\alpha'_y)}{a_{1f}\,(1 + \alpha'^2_y)^{1/2}}, \quad \text{where } \dot{\alpha}_t \equiv \frac{\partial \alpha}{\partial t}, \alpha'_y \equiv \frac{\partial \alpha}{\partial y} \tag{2.3}$$

and $a_1 = (\gamma p_1/\rho_1)^{1/2}$ is the sound speed in the upstream gas. Conservation of mass and transverse momentum across the front yield

$$\rho_{1f}(u_{1f} - \dot{\alpha}_t - w_{1f}\alpha'_y) = \rho_{2f}(u_{2f} - \dot{\alpha}_t - w_{2f}\alpha'_y), \quad w_{1f} + u_{1f}\alpha'_y = w_{2f} + u_{2f}\alpha'_y. \tag{2.4}$$

The flow geometry is unbounded downstream. From now on we introduce the notation, $u \to \overline{u} + u$, $\rho \to \overline{\rho} + \rho$, $p \to \overline{p} + p$, where an overbar identifies the unperturbed flow in the referential frame of the shock wave, $\overline{\alpha} = \overline{w}_1 = \overline{w}_2 = 0$. The flow (u_1, w_1, p_1) is prescribed with a small Mach number, $|u_1|/\overline{a}_1 \ll 1$, $|u_1|/|w_1| = O(1)$, $p_1 = O(\overline{\rho}_1 |u_1|^2)$.

A better understanding is provided by the simplified analysis performed in the distinguished limit making the compressed gas flow strongly subsonic relative to the shock front, $\overline{M}_2 \equiv \overline{u}_2/\overline{a}_2 \ll 1$,

$$\overline{M}_1 \equiv \overline{u}_1/\overline{a}_1 \gg 1, \quad \overline{M}_1^2(\gamma - 1) = O(1). \tag{2.5}$$

A perturbation analysis is then performed using the small parameter $\epsilon \equiv \overline{M}_2 \ll 1$,

$$\epsilon \equiv \overline{u}_2/\overline{a}_2 \approx (\overline{a}_2/\overline{a}_1)/\overline{M}_1 = \overline{a}_2/\overline{u}_1 \ll 1, \quad \text{where } \overline{a}_2/\overline{a}_1 = O(1), \tag{2.6}$$

$$(\overline{a}_2/\overline{a}_1)^2 \approx [2 + (\gamma - 1)\overline{M}_1^2]/2, \quad \overline{u}_2/\overline{u}_1 = \overline{\rho}_1/\overline{\rho}_2 \approx \epsilon^2, \quad \overline{p}_2/\overline{p}_1 \approx \overline{M}_1^2 = O(1/\epsilon^2). \tag{2.7}$$

3. Linear analysis of the shock–vortex interaction

3.1. *Method*

When the turnover velocity is sufficiently small so that the amplitude of the wrinkles of the front are also small, $|\alpha'_y| < 1$, the first stage of the shock–vortex interaction is well described by a linear analysis, and (2.2)–(2.4) yield

$$\frac{p_{2f}}{\overline{p}_2} - \frac{p_{1f}}{\overline{p}_1} \approx 2\frac{(u_{1f} - \dot{\alpha}_t)}{\overline{u}_1}, \quad \frac{\rho_{2f}}{\overline{\rho}_2} - \frac{\rho_{1f}}{\overline{\rho}_1} = 2\,(\overline{a}_1/\overline{a}_2)^2\,\frac{(u_{1f} - \dot{\alpha}_t)}{\overline{u}_1}, \tag{3.1}$$

$$(u_{2f} - \dot{\alpha}_t) = (u_{1f} - \dot{\alpha}_t)b/\overline{M}_1^2, \quad w_{2f} \approx \overline{u}_1\alpha'_y + w_{1f}, \tag{3.2}$$

where $b \equiv [(\gamma - 1)\overline{M}_1^2/2 - 1]$ is a parameter of order unity and where terms of order ϵ^2 have been omitted for simplicity in the numerical factor on the right-hand side of the first equation in (3.1) and the second equation in (3.2). In the linear approximation, the flow of compressed gas is the sum of an isobaric shear flow (incompressible entropy–vorticity wave) and an acoustic wave,

$$u_2 = u_2^{(i)} + u_2^{(a)}, \quad w_2 = w_2^{(i)} + w_2^{(a)}, \quad \partial u_2^{(i)}/\partial x + \partial w_2^{(i)}/\partial y = 0, \tag{3.3}$$

$$p_2^{(i)} = 0, \quad p_2 = p_2^{(a)}. \tag{3.4}$$

The shear flow, $u_2^{(i)}(x, y, t)$, $w_2^{(i)}(x, y, t)$, is the solution of the linearized Euler equations without the pressure term. Therefore, it may be expressed in terms of its value at the front $u_{2f}^{(i)}(y, t)$, $u_{2f}^{(i)}(y, t)$,

$$u_2^{(i)}(x, y, t) = u_{2f}^{(i)}(y, t - x/\overline{u}_2), \quad w_2^{(i)}(x, y, t) = w_{2f}^{(i)}(y, t - x/\overline{u}_2). \tag{3.5}$$

These values are obtained from $u_{2f}(y,t)$ and $w_{2f}(y,t)$ given by the Rankine–Hugoniot conditions (3.2), by subtracting the acoustic flow,

$$u_{2f}^{(i)}(y,t) = u_{2f} - u_{2f}^{(a)}, \quad w_{2f}^{(i)}(y,t) = w_{2f} - w_{2f}^{(a)}. \tag{3.6}$$

Once the acoustic flow is known, the linear equation for evolution of the disturbances of the shock front is obtained from (3.5) by the incompressibility condition in (3.3). In principle, the linear analysis can be performed in the general case by using the Laplace transform formalism, see Huete Ruiz de Lira (2012). The sound wave generated by shock–vortex interaction has been analysed by Ribner (1985). The full problem is a complex free boundary problem. It may be solved analytically in the limit (2.5).

3.2. *Normal mode analysis*

It is worth briefly recalling first the result of the normal mode analysis initiated by D'Yakov (1954) and Kontorovich (1957) for studying the stability of planar shock fronts in any quiescent material,

$$u_{1f} = w_{1f} = p_{1f} = 0, \tag{3.7}$$

see the recent reviews by Clavin & Williams (2012) and Bates (2012). This will be useful in § 3.5 for the final dynamics of the shock front after the vortex has crossed the shock wave. The flow and shock front are decomposed in transverse Fourier modes, $\mathrm{e}^{\mathrm{i}ky+\sigma t}$, which are analysed separately, $\alpha(y,t) = \tilde{\alpha}_k \mathrm{e}^{\mathrm{i}ky+\sigma t}$, $\alpha_y' = \mathrm{i}k\alpha$, $\dot{\alpha}_t = \sigma\alpha$ where k is real and σ complex. For each mode, the acoustic flow $(u_2^{(a)}, w_2^{(a)})$ is expressed in terms of σ and k from the pressure at the front p_{2f} given in (3.1) where u_{1f} and p_{1f} are set equal to zero. The quantities u_{2f} and w_{2f} are expressed in terms of σ and k from (3.2). Using (3.6), incompressibility of the shear flow at the front, $-(\sigma/\overline{u}_2)u_{2f}^{(i)} + ikw_{2f}^{(i)} = 0$ then leads to an equation for the reduced linear growth rate, $\sigma/\overline{a}_2|k|$,

$$\pm\,\overline{M}_2\sqrt{S^2+1} = 1 + S^2(1+1/\overline{M}_1^2), \quad \text{where } S \equiv (1-\overline{M}_2^2)^{-1/2}(\sigma/\overline{a}_2|k|). \tag{3.8}$$

For a polytropic gas the roots of (3.8) are purely imaginary and represent neutral normal modes (neither damped nor amplified exponentially in time). The square root in (3.8) is a pressure term. It introduces a cut in the complex S-plane which may lead to a relaxation characterized by power laws, as shown by using the Laplace transform formalism.

To leading order in the limit (2.5), according to (2.6), the pressure term, $\pm\overline{M}_2\sqrt{S^2+1}$, vanishes in (3.8). According to the relation $\overline{u}_1\overline{u}_2 \approx \overline{a}_2^2$ in (2.6), equation (3.8) then reduces to $S^2+1=0$, $\sigma^2+\overline{a}_2^2k^2=0$, that is a wave equation for the wrinkles of the front, $x=\alpha(y,t)$,

$$\ddot{\alpha}_{tt} - \overline{a}_2^2\alpha_{yy}'' = 0 \quad \text{with the notation } \ddot{\alpha}_{tt} \equiv \partial^2\alpha/\partial t^2, \quad \alpha_{yy}'' \equiv \partial^2\alpha/\partial y^2. \tag{3.9}$$

This shows that propagation of disturbances along the shock wave at velocity of sound is not necessarily associated with compressibility. The reason here is that the entropy–vorticity wave propagating in the compressed gas is strongly tilted, see figure 1. It is worth mentioning for the following and in particular for the calculations in § 4.1, that if the linear analysis is pushed to the next order in the limit (2.5), the pressure term, at this order, do not change the form of the wave equation (3.9) but only introduces a correction of order ϵ^2 to the phase velocity $\overline{a}_2$. This is easily seen

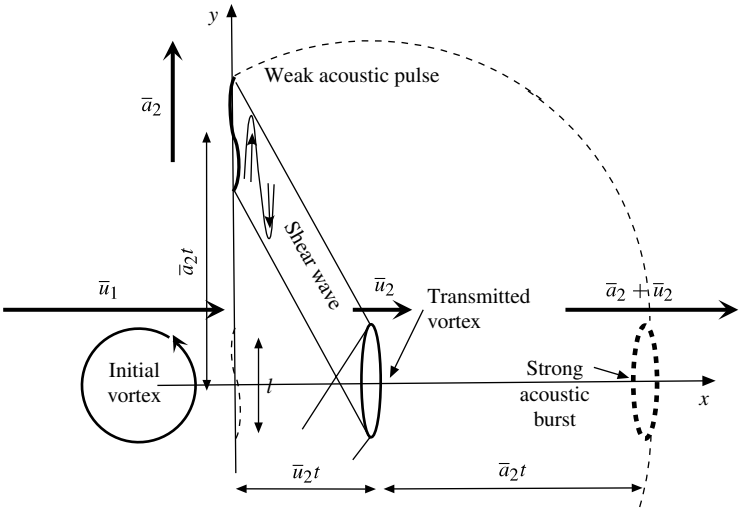

FIGURE 1. Sketch of the shock–vortex interaction, not drawn to scale, $\bar{u}_2/\bar{u}_1 \equiv \epsilon^2 \ll 1$, $\bar{u}_2/\bar{a}_2 = O(\epsilon)$ and $\bar{a}_2/\bar{u}_1 = O(\epsilon)$.

by noticing that the quantity $\sqrt{S^2+1}$ is of order ϵ, and the first term in (3.8) is of order ϵ^2.

3.3. *Shock–vortex cross-over (first stage)*

Coming back to the shock–vortex interaction, consider a rectilinear vortex of strength $\Gamma = 2\pi r_0 v_1$ where r_0 and $2v_1/r_0$ are the radius and the vorticity of the rotational core. The axis of the vortex is parallel to the planar shock front and perpendicular to the plan Oxy. The velocity of its centre, relative to the upstream gas, will be neglected compared with $\bar{u}_1$. The components $|u_1|$ and $|w_1|$ are of order v_1 near the core and decrease to zero with increasing radius r in the irrotational region ($r > r_0$), as $\Gamma/(2\pi r)$. This long tail makes the calculations of the shock–vortex interaction tedious, even though the small turnover velocities should be negligible. The analysis is carried out first with a simpler vortex model constituted by a blob of disturbances, $u_1(x, y)$, $w_1(x, y)$, of amplitude v_1 and finite extension l in space. The results are extended in § 3.7 to a variable length scale.

Introducing the finite size l, the perturbations of the upstream velocity $u_1(x, y)$ and $w_1(x, y)$ felt by the shock front are localized, $\Delta y = l$, and short-lived, $\Delta t = \tau_{int} \equiv l/\bar{u}_1$,

$$u_{1f}(y, t) = u_1(x, y)|_{x=-\bar{u}_1 t}, \quad w_{1f}(y, t) = w_1(x, y)|_{x=-\bar{u}_1 t}, \tag{3.10}$$

where $t = 0$ is the beginning of the shock–vortex cross-over. The time scale and length scale of this source term are

$$\partial/\partial t = O(\bar{u}_1/l), \quad \partial/\partial y = O(1/l). \tag{3.11}$$

Assuming, $\bar{u}_1 \gg \bar{a}_1 \gg v_1$, and neglecting the Doppler shift at leading order in the limit (2.5), $\bar{u}_2 \ll \bar{a}_2$, the linear equations of acoustics in the compressed gas yield,

$$\frac{\partial u_2^{(a)}}{\partial t} \approx -\frac{1}{\bar{\rho}_2}\frac{\partial p_2}{\partial x}, \quad \frac{\partial w_2^{(a)}}{\partial t} \approx -\frac{1}{\bar{\rho}_2}\frac{\partial p_2}{\partial y}, \quad \frac{\partial^2 p_2}{\partial t^2} - \bar{a}_2^2\left(\frac{\partial^2 p_2}{\partial x^2} + \frac{\partial^2 p_2}{\partial y^2}\right) \approx 0. \tag{3.12}$$

Sound generation by an impulsive source may be solved in free space by the method of Green's function, see for example the text book of Howe (2003). The acoustic waves propagating in the compressed gas are more complicated due to the free boundary at the shock front. Simplifications appear for a weak vortex and a strong shock in the limit (2.5). At low Mach number of turnover, $v_1/\overline{a}_1 \ll 1$, non-dimensional pressure and density disturbances, $p_1/\overline{p}_1$ and $\rho_1/\overline{\rho}_1$, are of order $(v_1/\overline{a}_1)^2$. Therefore, the upstream pressure fluctuation, p_{1f}, becomes negligible in the expression of the pressure disturbance at the compressed side in (3.1) for $v_1/\overline{a}_1 \ll \epsilon$,

$$v_1/\overline{a}_1 \ll \epsilon : \quad p_{2f}/\overline{p}_2 \approx 2(u_{1f} - \dot{\alpha}_t)/\overline{u}_1. \tag{3.13}$$

The pressure pulse at the downstream side of the front then corresponds to the longitudinal component of the turnover velocity of the vortex. This suggests that the pressure burst propagating in the compressed gas is generated at the shock front by an impulsive source constituted by a longitudinal flow of transverse extension l and short lifetime τ_{int}. During this short lapse of time, to leading order, the pressure pulse takes the form of a quasi-planar and longitudinal acoustic flow, $u_2^{(a)} \approx p_2/\overline{\rho}_2\overline{a}_2$ with $\overline{p}_2 \approx \overline{\rho}_2\overline{a}_2^2$, so that, according to (3.13),

$$0 \leqslant t \leqslant \tau_{int} : \quad u_{2f}^{(a)}(y,t) \approx 2(\overline{a}_2/\overline{u}_1)(u_{1f} - \dot{\alpha}_t), \tag{3.14}$$

where, according to (2.6), $(\overline{a}_2/\overline{u}_1) \approx \epsilon$. The validity of (3.14) is checked from (3.12) when using the time scale and the transverse length scale in (3.11): the longitudinal length scale results from the balance of the two first terms in the third equation in (3.12),

$$\partial/\partial x = O(\epsilon^{-1}/l), \tag{3.15}$$

and (3.13) with the first equation in (3.12) then yields (3.14). The order of magnitude of the transverse component of the acoustic flow is obtained from (3.13) and the second equation in (3.12),

$$w_{2f}^{(a)} = O((\overline{a}_2/\overline{u}_1)^2(u_{1f} - \dot{\alpha}_t)), \tag{3.16}$$

showing that, to leading order, the acoustic wave is quasi-planar, $|w_2^{(a)}/u_2^{(a)}| = O(\epsilon)$.

In the linear approximation the shear flow propagating in the compressed gas is given by (3.5) and (3.6). Neglecting terms of order ϵ^2, equations (3.2) and (3.14) yield

$$u_{2f}^{(i)}(y,t) \approx \dot{\alpha}_t(y,t) - 2(\overline{a}_2/\overline{u}_1)u_{1f}(y,t), \quad w_{2f}^{(i)}(y,t) = \overline{u}_1\alpha'_y + w_{1f} - w_{2f}^{(a)}, \tag{3.17}$$

where the order of magnitude of $w_{2f}^{(a)}$ is given by (3.16). According to (3.10) and (3.5), the last term in the first equation in (3.17) yields a contribution to $u_2^{(i)}(x,y,t)$ which may be expressed in terms of the upstream component $u_1(x,y)$ in the form $-2(\overline{a}_2/\overline{u}_1)u_1(-\overline{u}_1(t - x/\overline{u}_2),\ y)$. Its derivative with respect to x gives

$$-2\frac{\overline{a}_2}{\overline{u}_2}\left(\frac{\partial u_1}{\partial x}\right)_{x=-\overline{u}_1 t} = 2\frac{(\overline{a}_2/\overline{u}_1)}{\overline{u}_2}\frac{\partial\left(u_1|_{x=-\overline{u}_1 t}\right)}{\partial t}. \tag{3.18}$$

Incompressibility of the shear flow, $\partial u_2^{(i)}/\partial x + \partial w_2^{(i)}/\partial y = 0$, written at $x = 0$, leads to an equation for evolution of the front, valid during cross-over $0 \leqslant t \leqslant \tau_{int}$. Equation (3.17)

then yield

$$0 \leqslant t \leqslant \tau_{int}:$$
$$-\frac{\ddot{\alpha}_{tt}}{\overline{u}_2} + 2\frac{(\overline{a}_2/\overline{u}_1)}{\overline{u}_2}\frac{\partial\left(u_1|_{x=-\overline{u}_1 t}\right)}{\partial t} + \overline{u}_1\alpha''_{yy} - \left(\frac{\partial u_1}{\partial x}\right)_{x=-\overline{u}_1 t} - \frac{\partial w_{2f}^{(a)}}{\partial y} = 0, \quad (3.19)$$

where incompressibility of the upstream vortex flow, $\partial u_1/\partial x + \partial w_1/\partial y = 0$, has been used in the fourth term. Three terms are in fact negligible in this equation. According to (3.18) and $\overline{u}_2/\overline{a}_2 = \epsilon \ll 1$, see (2.6), the fourth term gives a correction of order ϵ to the second term. The latter is a source terms of order $\epsilon^{-1}u_{1f}/l$ which varies on the short time scale $\tau_{int} = l/\overline{u}_1$. According to (3.16), $\partial w_{2f}^{(a)}/\partial y = O(\epsilon^2(u_{1f} - \dot{\alpha}_t)/l)$, the last term in (3.19), yields contributions smaller than the second and first terms by a factor ϵ^3 and ϵ^4, respectively, since, according to (3.11), $\ddot{\alpha}_{tt}/\overline{u}_2 = O(\epsilon^{-2}\dot{\alpha}_t/l)$. Finally, the third term is smaller than the first term by a factor ϵ^2. Therefore, to leading order, the two first terms of (3.19) must be balanced, to give after integration with respect to time

$$0 \leqslant t \leqslant \tau_{int}: \quad \dot{\alpha}_t \approx 2\frac{\overline{a}_2}{\overline{u}_1}u_{1f}, \quad u_{1f} \equiv u_1|_{x=-\overline{u}_1 t}, \quad \alpha(y,t) \approx 2\frac{\overline{a}_2}{\overline{u}_1}\int_{-\overline{u}_1 t}^{0} \mathrm{d}x\frac{u_1(x,y)}{\overline{u}_1}. \quad (3.20)$$

3.4. *Orders of magnitude*

As already mentioned, the fourth term in (3.19) is the first correction term, of order ϵ, to the two first terms, so that $\partial w_{2f}^{(i)}/\partial y \approx \partial w_{1f}/\partial y$ and $w_{2f}^{(i)} \approx w_{1f}$. According to (3.5) and (3.11),

$$\partial u_2^{(i)}/\partial x = -\overline{u}_2^{-1}\partial u_2^{(i)}/\partial t = O((\overline{u}_1/\overline{u}_2)(u_2^{(i)}/l)). \quad (3.21)$$

Incompressibility of the shear wave written in the form $\partial u_2^{(i)}/\partial x \approx -\partial w_{1f}/\partial y$ then shows that $|u_2^{(i)}/w_{1f}| = O(\overline{u}_1/\overline{u}_2)$, namely, using (2.6), $|u_2^{(i)}/w_2^{(i)}| = O(\epsilon^2)$.

For a single vortex blob, the quantity under the integral in (3.20), $u_1(x,y)$, does not change sign at y fixed but changes sign when crossing $y = 0$. According to (3.20), the amplitude of the wrinkle, $|\alpha|$, left just after the passage of the vortex of size l, is of order $\epsilon l v_1/\overline{u}_1$ since $\overline{a}_2/\overline{u}_1 \approx \epsilon$, see (2.6). Therefore, the slope of the wrinkled front $|\alpha'_y|$ is small, of order $\epsilon v_1/\overline{u}_1 = \overline{a}_2 v_1/\overline{u}_1^2$. The corrugation of the wrinkled front, $x = \alpha(y)$, changes sign when crossing $y = 0$, $\alpha(y = 0) = 0$. Its amplitude decreases when increasing $|y|$ and is zero for $|y| > l/2$.

Therefore, the physical interpretation of the shock–vortex interaction during the cross-over is simple for $v_1/\overline{a}_1 \ll \epsilon$ in the limit (2.5):

(i) the acoustic pulse is generated by the longitudinal component of the turnover velocity of the vortex;

(ii) the shear flow is generated by the transverse component of the vortex and is quasi-parallel to the front; this flow corresponds to the transmitted vortex core.

The result, which is based on the approximation in (3.13)–(3.14), may be summarized as follows:

$$(v_1/\overline{a}_1) \ll \epsilon, \quad 0 \leqslant t \leqslant \tau_{int}:$$
$$\dot{\alpha}_t \approx 2\epsilon u_{1f}, \quad |\alpha'_y| = O(\epsilon v_1/\overline{u}_1), \quad (3.22)$$
$$p_{2f}/\overline{p}_2 \approx 2u_{1f}/\overline{u}_1, \quad u_{2f}^{(a)} \approx 2\epsilon u_{1f}, \quad |w_{2f}^{(a)}/u_{2f}^{(a)}| = O(\epsilon), \quad (3.23)$$
$$w_{2f}^{(i)} \approx w_{1f}, \quad |u_{2f}^{(i)}/w_{2f}^{(i)}| = O(\epsilon^2). \quad (3.24)$$

If $v_1/\overline{a}_1$ is still small but becomes of order ϵ, equation (3.20) should be modified to take into account the pressure inside the vortex, $u_{1f} \to u_{1f} + \epsilon^{-1} p_{1f}/(2\overline{\rho}_1 \overline{a}_2)$,

$$v_1/\overline{a}_1 = O(\epsilon), \quad 0 \leqslant t \leqslant \tau_{int} : \quad \dot{\alpha}_t = O(u_{1f}^2/\overline{a}_2), \quad |\alpha_y'| = O(\epsilon v_1^2/(\overline{a}_1 \overline{u}_1)). \quad (3.25)$$

However, the approximation in (3.14) is less accurate in this case.

3.5. *Linear evolution after the cross-over (second stage)*

For $t > \tau_{int}$, the pressure pulse becomes multidimensional. For weak shock, it takes a quasi-cylindrical shape in the far field, centred on the transmitted vortex core, as sketched in figure 1, see Ribner (1985), Inoue & Hattory (1999), Inoue (2000) and Zhang *et al.* (2005). However, for a weak vortex and a strong shock in the limit (2.5), the sound intensity varies with the azimuthal angle and decreases to negligible values when approaching the shock front ($x = 0, \ |y| > l/2$). The dynamic of the wrinkled shock front after the vortex has crossed the shock wave is mainly controlled by a quasi-isobaric flow in the compressed gas, as shown now. During the second stage ($t > \tau_{int}$), the acoustic flow at the downstream side of the compressed gas may be decomposed into two parts:

(i) the acoustic waves radiated from the flow disturbances propagating in the compressed gas and which were generated initially during the short period τ_{int};

(ii) the pressure fluctuations generated at the shock front by the wrinkles propagating along the shock front after τ_{int}.

Consider to begin with the first mechanism. For a cylindrical vortex, the longitudinal component of the upstream velocity disturbance at the front, $u_{1f}(y, t)$, is antisymmetric, $u_{1f}(y, t) = -u_{1f}(-y, t)$, it does not change sign neither for $y > 0$ nor during its lifetime τ_{int}, and it vanishes for $|y| > l/2$. According to (3.23), this is also true for the longitudinal impulsive flow, $u_{2f}^{(a)}(y, t)$, which generates the acoustics pulse propagating afterwards in the shocked gas, $t > \tau_{int}$. Therefore, due to the longitudinal character of the flow of the impulsive source, the directivity of the pressure pulse in the far field (large distance compared with l) is oriented downstream along the x-axis, so that this acoustic field does not perturb the shock front ($x = 0, \ |y| > l/2$) for $t > \tau_{int}$. Consider now the second mechanism. Neglecting the acoustic disturbance radiated from the compressed gas and in the absence of upstream disturbances, $p_{1f} = u_{1f} = w_{1f} = 0$, the situation is similar to that of the normal mode analysis. According to (3.1) with $p_{1f} = 0$, $p_{2f}/\overline{\rho}_2 \approx -2(\overline{a}_2^2/\overline{u}_1)\dot{\alpha}_t$, the flow velocity of the resulting acoustic wave is of order $(\overline{a}_2/\overline{u}_1)\dot{\alpha}_t$. According to (3.9), the wrinkles propagate in the transverse direction with the sound speed of the compressed gas, $|\dot{\alpha}_t| = O(\overline{a}_2|\alpha_y'|)$, so that, to leading order in the limit (2.5), the flow of the acoustic waves near the front in the shocked gas is parallel to the unperturbed front. The flow velocity of this acoustic wave being of order $(\overline{a}_2/\overline{u}_1)\dot{\alpha}_t = O\left((\overline{a}_2^2/\overline{u}_1)|\alpha_y'|\right)$, it is smaller by a factor ϵ^2 than the transverse component of the velocity $w_{2f} = \overline{u}_1 \alpha_y'$ given by (3.2) with $w_{1f} = 0$. It is thus negligible at the leading order in the limit (2.5).

To summarize, according to (3.2), $u_{2f}^{(i)} \approx \dot{\alpha}_t$, $w_{2f}^{(i)} \approx \overline{u}_1 \alpha_y'$, and (3.5)–(3.6) for a negligible acoustic flow, the shear flow takes the form

$$t > \tau_{int} : \quad u_2^{(i)}(x, y, t) \approx \dot{\alpha}_t(y, t - x/\overline{u}_2), \quad w_2^{(i)}(x, y, t) \approx \overline{u}_1 \alpha_y'(y, t - x/\overline{u}_2), \quad (3.26)$$

Incompressibility, $\partial u_2^{(i)}/\partial x + \partial w_2^{(i)}/\partial y = 0$ and the relation $\overline{u}_1 \overline{u}_2 \approx \overline{a}_2^2$ in (2.6), then show that the linear dynamics of the wrinkles after the cross-over is effectively controlled by the wave equation of the normal modes (3.9). This equation corresponds to the first

and third terms in (3.19). The time scale of the second stage is thus longer than that of the first stage, τ_{int}, by a factor ϵ^{-1}, $l/\bar{a}_2 = O(\tau_{int}/\epsilon)$, and the order of magnitudes are

$$t > \tau_{int}: \quad |\dot{\alpha}_t| = O(\bar{a}_2|\alpha'_y|), \quad w^{(i)}_{2f} \approx \bar{u}_1\alpha'_y, \quad |u^{(i)}_{2f}/w^{(i)}_{2f}| = O(\epsilon), \tag{3.27}$$

$$|w^{(a)}_{2f}/w^{(i)}_{2f}| = O(\epsilon^2), \quad |u^{(a)}_{2f}/w^{(a)}_{2f}| = O(\epsilon), \tag{3.28}$$

where $|\alpha'_y| = O(\epsilon v_1/\bar{u}_1)$ is given by the first stage, see (3.22). The second relation in (3.28) is obtained from the linear solution of the normal modes, see for example Clavin & Williams (2012).

According to (3.9) and (3.19), a composite equation for the linear evolution of the front takes the simple form of a wave equation with a forcing term,

$$v_1/\bar{a}_1 \ll \epsilon: \quad \ddot{\alpha}_{tt} - \bar{a}_2^2\alpha''_{yy} = 2(\bar{a}_2/\bar{u}_1)\partial u_{1f}/\partial t. \tag{3.29}$$

If $v_1/\bar{a}_1$ is of order ϵ, $1 \gg (v_1/\bar{a}_1) \geqslant \epsilon$, equation (3.29) is still valid with a different forcing term, $u_{1f} \to u_{1f} + \epsilon^{-1}p_{1f}/(2\bar{\rho}_1\bar{a}_2)$, still localized in space, $\Delta y/l = 1$, and time, $\Delta t/\tau_{int} = 1$, see (3.25).

3.6. *Simple waves*

After the cross-over the disturbances of the front take the form of two simple waves,

$$t > \tau_{int}: \quad \alpha(y, t) = A_-(y - \bar{a}_2 t) + A_+(y + \bar{a}_2 t), \tag{3.30}$$

where the functions $A_\pm(y)$ are determined by (3.29) and are zero for $|y| > l/2$. According to (3.20), $A_\pm(y)$ should not be much different from $(\bar{a}_2/\bar{u}_1)\int \mathrm{d}x u_1(x, y)/\bar{u}_1$ for $v_1/\bar{a}_1 \ll \epsilon$. The transverse component of the shear flow is given by the second equation in (3.26) and (3.30), see also figure 1. The transverse component of the shear flow in (3.26) is proportional either to $A'_-(y - \bar{a}_2 t + x/\epsilon)$ or to $A'_+(y + \bar{a}_2 t - x/\epsilon)$, depending on the simple wave from which they are generated. These two flows merge in a thin region, $\Delta x = \epsilon l$, $\Delta y = l$, centred on the x-axis near $x \approx \bar{u}_2 t$. This thin overlapping region includes the transmitted vortex which is constituted by the strong shear wave which was generated during the cross-over $0 < t < \tau_{int}$, $w_{1f}(-\bar{u}_1(t - x/\bar{u}_2), y)$, see (3.5), (3.24) and figure 1. After a time lapse $\Delta t > l/\bar{u}_2$, the two simple waves are separated by the distance $\Delta y > l/\epsilon$ and the shear flows do not overlap in the vicinity of the front, in a region larger than l, $\Delta x > l$, as shown in figure 1.

3.7. *Rectilinear vortex with an irrotational tail*

Outside the rotational core, the length scale of the irrotational flow in a rectilinear vortex varies as the distance r from the centre. This does not change the analysis and (3.29), in which the length scale l does not appear explicitly, is still valid. At a distance from the vortex centre of the order of the core radius, $r/r_0 = O(1)$, the length scale is fixed, $l \approx r_0$, and the situation is the same as in § 3.5. This corresponds to the central part of the simple waves in (3.30) where the slope $|\alpha'_y|$ is maximum, $|y| \lesssim l$ for $|A(y)|$. However, the simple waves have wings associated with the tails of the irrotational flow in the vortex, $r > l$, $|y| > l$ for $|A(y)|$. The time and length scales increases in the wings with the distance from the centre of the simple wave. These wings do not play significant roles, because the wave breaking studied in § 4.2 concerns the vicinity of the maximum of slope $|\alpha'_y|$. At leading order in the limit (2.5), the wings are fully negligible as soon as they are produced by turnover velocities smaller than v_1 by a factor ϵ. According to the vortex structure $v/v_1 \approx r_0/r$, this occurs at a distance from the centre of order r_0/ϵ. Therefore, the transverse extension

of the simple waves is $l \approx r_0/\epsilon$ but the time scale of the front wrinkles in the central part of the simple waves is $r_0/\overline{a}_2$. For $\Delta t > \epsilon^{-1} r_0/\overline{u}_2$, the x-extension of the non-overlapping region discussed in § 3.6 is larger than the transverse extension of the simple waves.

4. Weakly nonlinear analysis

In this section, we perform a weakly nonlinear analysis for $t > l/\overline{a}_2$, more precisely for $t = O(\epsilon^{-1} r_0/\overline{u}_2)$. The objective is to see whether singularities appear in the long time limit. The method is similar to that developed by Clavin (2002*a*) for studying cellular detonations, see also Clavin (2002*b*).

4.1. *Nonlinear equation for the evolution of the shock front*

According to (2.1), conservation of momentum takes the form,

$$\frac{\partial u_2}{\partial t} + \overline{u}_2 \frac{\partial u_2}{\partial x} = U - \frac{1}{\rho_2}\frac{\partial p_2}{\partial x}, \quad \frac{\partial w_2}{\partial t} + \overline{u}_2 \frac{\partial w_2}{\partial x} = W - \frac{1}{\rho_2}\frac{\partial p_2}{\partial y}, \tag{4.1}$$

where $U \equiv u_2 \partial u_2/\partial x + w_2 \partial u_2/\partial y$ and $W \equiv u_2 \partial w_2/\partial x + w_2 \partial w_2/\partial y$. A perturbation method may be used if the quadratic terms U and W are small compared with the unsteady terms. When expressed in terms of (3.26), the quadratic terms take the form

$$U \approx \frac{1}{2}\frac{\partial H}{\partial x}, \quad W \approx -\frac{1}{2}\frac{\overline{u}_1}{\overline{u}_2}\frac{\partial H}{\partial y}, \quad H \equiv [-\dot{\alpha}_t'^2(t - x/\overline{u}_2, y) + \overline{a}_2^2 \alpha_y'^2(t - x/\overline{u}_2, y)], \tag{4.2}$$

where $\overline{u}_2\overline{u}_1 \approx \overline{a}_2^2$ has been used. According to (3.26) and (3.27), these terms introduce small corrections to the leading order of the linear dynamics of order $\varepsilon \equiv |\alpha_y'|/\epsilon$. According to (3.28), acoustic terms in the quadratic terms would introduce smaller corrections, smaller at least by a factor ϵ. Therefore, U and W in (4.2) are the dominant nonlinear terms in the Euler equations (4.1). For shock–vortex interaction in the limit (2.5), the order of magnitude of the small parameter ε depends on the turnover velocity v_1,

$$\varepsilon = O(v_1/\overline{u}_1) \quad \text{for } v_1/\overline{a}_1 \ll \epsilon \quad \text{or} \quad \varepsilon = O(v_1^2/(\overline{u}_1\overline{a}_1)) \quad \text{for } v_1/\overline{a}_1 = O(\epsilon), \tag{4.3}$$

see (3.22) and (3.25). Introducing (3.30) into (4.2), H takes the form of a product of simple waves $H = -4A_-'(y - \overline{a}_2 t + x/\epsilon)A_+'(y + \overline{a}_2 t - x/\epsilon)$. Therefore, in the long time limit, according to § 3.6, the terms U and W are negligible in a wide downstream domain, adjacent to the front, see figure 1, so that they do not influence the dynamics of the front at order ε of the perturbation analysis.

However, quadratic terms appear also in the boundary conditions and introduce corrections of order ε to the linear dynamics. Taking into account of the quadratic terms, equations (2.2)–(2.4) yield

$$p_{2f}/\overline{p}_2 = -2\dot{\alpha}_t/\overline{u}_1 - \alpha_y'^2, \quad (u_{2f} - \dot{\alpha}_t)(1 - \kappa\dot{\alpha}_t/\overline{u}_1) = w_{2f}\alpha_y', \quad w_{2f} = \overline{u}_1\alpha_y' - u_{2f}\alpha_y', \tag{4.4}$$

where $\kappa \equiv 2\,(\overline{a}_1/\overline{a}_2)^2$ is a parameter of order unity, and where corrections of order ϵ^2 have been neglected for simplicity. In principle, terms of order ϵ^2 would have to be retained in the weakly nonlinear of the shock vortex interaction, since, according to (4.3), $\epsilon^2 > \varepsilon$. As in the study of cellular detonations by Clavin & Denet (2002) this would not change the nonlinear dynamics but introduce useless corrections in the coefficients of the linear operator, see the end of § 3.2. In order to simplify the presentation these terms are not retained in the following calculations. The

corresponding small quantitative correction may be easily introduced afterwards in the final result.

It is more convenient in the nonlinear analysis to introduce a system of coordinates attached to the front,

$$\left.\begin{array}{l} \xi = x - \alpha(y,t), \quad \partial/\partial t \to \partial/\partial t - \dot{\alpha}_t \partial/\partial\xi, \quad \partial/\partial y \to \partial/\partial y - \alpha'_y \partial/\partial\xi, \\ \partial/\partial x \to \partial/\partial\xi. \end{array}\right\} \tag{4.5}$$

The boundary conditions in (4.4) concern $\xi = 0$, but the change of referential introduces new quadratic terms in the equations. From now on, we will use the flow splitting,

$$p_2 = p_2^{(a)} + \tilde{p}, \quad u_2 = u_2^{(a)} + \tilde{u}, \quad w_2 = w_2^{(a)} + \tilde{w} \tag{4.6}$$

where the acoustical flow is smaller than the linear part by a factor ϵ^2, see (3.28). Neglecting the nonlinear acoustic terms and introducing (3.26) into the quadratic terms, the Euler equations (4.1) yield

$$\frac{\partial\tilde{u}}{\partial\xi} + \frac{\partial\tilde{w}}{\partial y} = \tilde{X}, \quad \frac{\partial\tilde{u}}{\partial t} + \overline{u}_2\frac{\partial\tilde{u}}{\partial\xi} = \tilde{U} - \frac{1}{\overline{\rho}_2}\frac{\partial\tilde{p}}{\partial\xi}, \quad \frac{\partial\tilde{w}}{\partial t} + \overline{u}_2\frac{\partial\tilde{w}}{\partial\xi} = \tilde{W} - \frac{1}{\overline{\rho}_2}\frac{\partial\tilde{p}}{\partial y}, \tag{4.7}$$

$$\text{where } \tilde{U} \equiv -\dot{\alpha}_t(y,t)\ddot{\alpha}_{tt}(y, t-\xi/\overline{u}_2)/\overline{u}_2, \quad \tilde{W} \equiv -(\overline{u}_1/\overline{u}_2)\dot{\alpha}_t(y,t)\dot{\alpha}'_{ty}(y, t-\xi/\overline{u}_2) \tag{4.8}$$

$$\text{and } \tilde{X} \equiv -(\overline{u}_1/\overline{u}_2)\alpha'_y(y,t)\dot{\alpha}'_{ty}(y, t-\xi/\overline{u}_2). \tag{4.9}$$

The first equation in (4.7) means that the flow $(\tilde{u}, \tilde{w})$ is incompressible. The acoustic pressure being excluded from the pressure term, $\tilde{p}$ is a quadratic term which should be at least of order $\overline{\rho}_2 \left(w_2^{(i)}\right)^2 \approx \overline{\rho}_2 \overline{u}_1^2 \alpha_y'^2$ to be non-negligible. Using (3.9) and the relation $\overline{a}_2^2 \approx \overline{u}_1\overline{u}_2$ in (2.6), one gets, according to the definitions of $\tilde{U}$, $\tilde{W}$ and $\tilde{X}$ in (4.8)–(4.9),

$$\partial\tilde{U}/\partial\xi + \partial\tilde{W}/\partial y = \partial\tilde{X}/\partial t + \overline{u}_2\partial\tilde{X}/\partial\xi. \tag{4.10}$$

Introducing (4.10) into (4.7) show that $\tilde{p}$ is a solution of Laplace's equation,

$$\partial^2\tilde{p}/\partial\xi^2 + \partial^2\tilde{p}/\partial y^2 = 0. \tag{4.11}$$

Equation (4.7) and (4.11) are valid except in the thin overlapping layer at $x = \overline{u}_2 t$ mentioned in § 3.6. In the long time limit, this overlapping zone is sufficiently far away downstream from the shock front, so that it can no longer influence the shock dynamics. Therefore, according to Laplace's equations (4.11), the pressure term $\tilde{p}$ could be generated only from the nonlinear terms in the boundary condition (4.4) at the shock. However, the quadratic term in the first equation in (4.4) gives a negligible contribution to $\tilde{p}$, of order $\overline{\rho}_2\overline{a}_2^2\alpha_y'^2$, smaller than $\overline{\rho}_2\left(w_2^{(i)}\right)^2$ by a factor ϵ^2. Therefore, the flow $(\tilde{u}, \tilde{w})$ is a solution of (4.7) with $\tilde{p} = 0$. Retaining the corrections of order $\varepsilon \approx |\alpha'_y|/\epsilon$ and neglecting correction of order ϵ^2, the boundary conditions in (4.4) reduce to

$$\epsilon^3 < |\alpha'_y| < \epsilon \Rightarrow \xi = 0: \quad \tilde{u} = \tilde{u}_f(y,t) \equiv \dot{\alpha}_t + \overline{u}_1\alpha_y'^2, \quad \tilde{w} = \tilde{w}_f(y,t) \equiv \overline{u}_1\alpha'_y. \tag{4.12}$$

The solutions to the second and third equation in (4.7) for $\tilde{p} = 0$, subject to the boundary condition (4.12), are obtained by noticing that every function of t and ξ through the grouping $t - \xi/\overline{u}_2$ is a solution to the corresponding equations without the

second member,

$$\tilde{u} = \tilde{u}_f(y, t - \xi/\overline{u}_2) + \tilde{\mathscr{U}}(\xi, y, t), \quad \tilde{w} = \tilde{w}_f(y, t - \xi/\overline{u}_2) + \tilde{\mathscr{W}}(\xi, y, t), \tag{4.13}$$

$$\text{where } \tilde{\mathscr{U}} \equiv [\alpha(y, t - \xi/\overline{u}_2) - \alpha(y, t)]\ddot{\alpha}_{tt}(y, t - \xi/\overline{u}_2)/\overline{u}_2, \tag{4.14}$$

$$\tilde{\mathscr{W}} \equiv (\overline{u}_1/\overline{u}_2)[\alpha(y, t - \xi/\overline{u}_2) - \alpha(y, t)]\dot{\alpha}'_{yt}(y, t - \xi/\overline{u}_2). \tag{4.15}$$

The flow $(\tilde{\mathscr{U}}, \tilde{\mathscr{W}})$ is incompressible, $\partial\tilde{\mathscr{U}}/\partial\xi + \partial\tilde{\mathscr{W}}/\partial y = \tilde{X}$, as is checked by using (3.9) and the relation $H = 0$, $\dot{\alpha}_t^2 = \overline{a}_2^2\alpha_y'^2$. Incompressibility of the flow $(\tilde{u}, \tilde{w})$, the first equation in (4.7), then leads to a nonlinear wave equation of the shock front,

$$\epsilon^3 < |\alpha'_y| < \epsilon, \quad t = O(\epsilon^{-1}r_0/\overline{u}_2): \qquad \frac{\partial^2\alpha}{\partial t^2} - \overline{a}_2^2\frac{\partial^2\alpha}{\partial y^2} + \overline{u}_1\frac{\partial}{\partial t}\left[\left(\frac{\partial\alpha}{\partial y}\right)^2\right] = 0, \tag{4.16}$$

where the lower bound of $|\alpha'_y|$ is the condition for the acoustic effects of order ϵ^2 to be negligible in the linear operator. As already mentioned, when the compressible terms of order ϵ^2 are taken into account, the form of the equation in (4.16) is not changed, but simply a useless correction of order ϵ^2 is introduced into the phase velocity $\overline{a}_2$. Therefore, the lower bound of $|\alpha'_y|$ may be suppressed and (4.16) is valid for the second stage of the interaction of a weak vortex and a strong shock in the limit (2.5).

4.2. *Mach stem formation*

The nonlinear term in (4.16) introduces corrections to $\dot{\alpha}_t \approx \pm\overline{a}_2\alpha'_y$ of order $\varepsilon \approx |\alpha'_y|/\epsilon$. Introducing the non-dimensional quantities $\eta = y/r_0$, $\tau = \overline{a}_2 t/r_0$, and $\mathscr{A} = \alpha/(\varepsilon\epsilon r_0)$, equation (4.16) takes the form of a two-time-scale equation, involving the parameter ε

$$\varepsilon \ll 1, \quad \mathscr{A} = O(1), \quad \tau = O(1),: \qquad \frac{\partial^2\mathscr{A}}{\partial\tau^2} - \frac{\partial^2\mathscr{A}}{\partial\eta^2} + \varepsilon\frac{\partial}{\partial\tau}\left[\left(\frac{\partial\mathscr{A}}{\partial\eta}\right)^2\right] = 0. \tag{4.17}$$

Equation (4.17) may be transformed into an equation free from parameters by introducing $\tilde{\mathscr{A}} = \varepsilon\mathscr{A}$. However, the form of (4.17) is convenient to show that the solutions have breaking waves. For any smooth initial data, $\mathscr{A}(\eta, \tau = 0) = O(1)$, $\partial\mathscr{A}/\partial\eta = O(1)$, vanishing at large distance, $|\eta| \to \infty$, the derivative $\partial\mathscr{A}/\partial\eta$ develops a jump discontinuity in finite time, $\tau = O(1/\varepsilon)$, and the front develops a corner, representative of Mach stem formation. This is easily seen by introducing the slow time scale $\tau' = \varepsilon\tau$, and focusing attention on simple waves, $\mathscr{A} = \mathrm{A}(\eta', \tau')$ where $\eta' = \eta \pm \tau$. To leading order in an expansion for small ε, equation (4.17) leads to the Burgers' equation for the slope,

$$\partial\mathrm{A}'/\partial\tau' + \mathrm{A}'\partial\mathrm{A}'/\partial\eta' = 0, \quad \text{where } \mathrm{A}'(\eta, \tau) \equiv \partial\mathrm{A}/\partial\eta'. \tag{4.18}$$

This shows Mach stem formation in the limit (2.5).

4.3. *Composite solution*

Neglecting the nonlinear effects during the short time of cross-over, a composite equation for the shock–vortex interaction is obtained by combining (3.29) and (4.16), that is by introducing the forcing term $\overline{a}_2\partial\pi/\partial t$ on the right-hand side of (4.16) with $\pi(y, t) \equiv 2(u_{1f}/\overline{u}_1) + p_{1f}/(\overline{\rho}_1\overline{a}_2^2)$. This term varies on the short time scale of cross-over, shorter than the characteristic scale of the travelling wave. Using the same reduced variables τ and η as in (4.17) and introducing $\tilde{\mathscr{A}} = \varepsilon\mathscr{A}$, the equation for the two-dimensional shock front takes the form

$$(v_1/\overline{a}_1) \ll 1: \quad \partial^2\tilde{\mathscr{A}}/\partial\tau^2 - \nabla^2\tilde{\mathscr{A}} + \partial\left|\nabla\tilde{\mathscr{A}}\right|^2/\partial\tau = \mathscr{H}, \tag{4.19}$$

where the forcing term is $\mathscr{H}(\eta,\tau)\equiv\epsilon^{-1}\partial\pi/\partial\tau$, $\eta\in\mathbb{R}^2$. The pressure term in π coming from the upstream pressure fluctuation p_{1f} is retained in order to take into account the vortices whose strength is of order ϵ, see (3.25), and not only smaller than ϵ as in (3.22)–(3.24). However, in this case, the directivity of the pressure pulse mentioned in § 3.5 is less pronounced and the quasi-isobaric approximation less accurate.

For a single vortex the function $\pi(y,t)$ is non-zero for a space extension of the order of r_0 and for a short period of time, $\Delta t=l/\overline{u}_1\approx r_0/\overline{a}_1$. This corresponds to a stiff forcing term in (4.19) $\mathscr{H}(\eta,\tau)=\epsilon^{-2}h(\eta,\epsilon^{-1}\tau)$ where $h(\eta,\cdot)$ is a function of order unity.

5. Discussion of the result, conclusions and perspectives

The present analysis shows that, to leading order in the limits (2.5), the formation of singularities of the slope of the weakly wrinkled front of a strong shock is mainly due to a geometrical term in the boundary conditions at the front. This nonlinear term, $w_{2f}\alpha_y'$, comes from the Rankine–Hugoniot condition (2.4) concerning the normal component of the flow velocity, see (4.4), (4.12) and (4.16). The other nonlinearities in the Euler equations controlling the flow in the compressed gas are not essential. In particular, the acoustic waves in the shocked gas do not influence the nonlinear dynamics in the limit (2.5). Their effect on the linear dynamics is limited to useless small quantitative corrections. Therefore, the dynamics of the shock front is mainly controlled by the incompressible flow of the shear waves generated by the front wrinkling. This last approximation is valid for the normal modes at the leading order in the limit (2.5). Its validity for the second stage ($t\gg\tau_{int}$) of the interaction of a strong shock and a weak vortex, $v_1\ll\overline{a}_1$, is discussed in § 3.5.

Even in the absence of compressible effects (acoustic waves), the wrinkles of the shock front propagate in the transverse direction at the sound velocity of the shocked gas, see (3.9) and (4.16)–(4.19). This is due to the fact that the incompressible shear waves (vorticity waves), which propagate into the shocked gas with a longitudinal component of velocity equal to the subsonic velocity of the flow velocity, $x=\overline{u}_2t$, $\overline{u}_2=\epsilon\overline{a}_2$, are strongly tilted in the transverse direction, $y=\pm x/\epsilon$, see figure 1 and the text below (3.30), $A'_{\pm}(y\pm\overline{a}_2t\mp x/\epsilon)$. This shows that transverse propagation of the wrinkles at the sound speed, $y=\mp\overline{a}_2t$, is not necessary associated with acoustic waves.

Equations (4.16) and (4.17) are the same as the nonlinear equations obtained for the normal modes at the leading order in the limit (2.5). The solution breaks down after a finite time and the slope of the front develops jump discontinuities, indicating the formation of Mach stems, as shown in § 4.2. The small acoustic waves, which appear near the shock front at the next order of the perturbation analysis, propagate in the quasi-parallel direction to the shock front. However, they are slightly non-radiating and the normal mode solution thus looks non-causal. This is not the case for the shock–vortex interaction because the non-radiating character is strictly local and limited to the vicinity of the shock front. The weakly non-radiating quasi-transverse acoustic waves which are associated with the wrinkles during the second stage, $t>\tau_{int}$, match the small acoustic waves that are radiated from the disturbances, generated earlier into the compressed gas flow, during the short interaction time, $0<t<\tau_{int}$. The global acoustic flow is radiated from the transmitted vortex, as shown in figure 1. Here, normal modes that do not satisfy the causality condition are useful in the dynamics of the shock front. This is a counterexample of usual cases for which such modes are not meaningful.

In the limit (2.5), the shock–vortex interaction takes the form of a two-time-scale problem, $\tau_{int} = l/\overline{u}_1 \ll l/\overline{a}_2$, involving wrinkles of the shock front of small amplitude. The simple form of the final result in (4.19) rests on the approximation in (3.14). The physical insights may be summarized as follows. To leading order, the transmitted vortex is associated with the transverse velocity w_1 of the initial vortex, $w_{2f}^{(i)} \approx w_{1f}$, while its longitudinal velocity, u_1, triggers the acoustic pulse which is generated by the cross-over during the short interaction time τ_{int}, $u_{2f}^{(a)} \approx 2\epsilon u_{1f}$, $|w_{2f}^{(a)}/u_{2f}^{(a)}| \ll 1$, see (3.22)–(3.25). The longitudinal character of the impulsive acoustic flow at the shock front implies that the directivity of the resulting acoustic pulse, which is sent into the shocked gas, is along the direction normal to the shock front. Therefore, to leading order in the limit (2.5), the acoustic pulse does not influence the second stage of the front dynamics ($t > \tau_{int}$, $x = 0$, $|y| > l/2$). Matching this pulse and the small acoustic flows that are generated at the wrinkled shock front after the cross-over ($t > t_{int}$), requires us to push the perturbation analysis to next orders. This is a difficult task, beyond the scope of the present analysis. Further works have to be performed in that direction. Another consequence of (3.14) is that the transmitted vortex is reduced to a thin isobaric shear wave (of thickness $l\overline{u}_2/\overline{u}_1 \approx \epsilon^2 l$), elongated in the transverse direction and propagating in the normal direction at the velocity of the compressed gas flow $\overline{u}_2$, see figure 1.

The main role of the source term in the right-hand side of (4.19) is limited to control the initial amplitude of the wrinkles which are initially produced during the short interaction time τ_{int}. The full structure of the Mach stem cannot be described without solving the acoustic problem. However, after introducing artificially a small damping term for transforming the singularities into sharp folds, equation (4.19) may be used to model the geometry of the cusped surface of a shock front propagating in a turbulent flow, viewed as an ensemble of vortices. The stiffness of the forcing term results from the fact that the interaction time of each vortex is shorter than the time necessary for the nonlinear term in the left-hand side of (4.19) to produce sharp folds. A too high frequency of the disturbances of the shock front may not leave a sufficient long time for formation of sharp folds. Therefore, in the limit (2.5), the formation of folds looks to be favoured by the intermittency of the turbulent flow with short-lived bursts of order $l/\overline{u}_1$, followed by longer quasi-laminar periods, of order $l/\overline{a}_2$. In that respect, numerical analyses of a regularized version of (4.19) may be useful to improve our understanding of the geometry of a two-dimensional shock front propagating in a three-dimensional turbulent flow.

The present analysis works neither for weak shocks, $(\overline{M}_1 - 1) < 1$, nor for strong vortex ($v_1/\overline{a}_1$ not sufficiently smaller than unity). In these cases the acoustic waves influences the front dynamics. However the wrinkles of the shock front still propagate in the transverse direction at a velocity close to the sound velocity in the compressed gas. If the dominant nonlinear term is similar to that in (4.19), as is the case in the analysis of reactive shock fronts by Majda & Rosales (1983), the end result could not be much different from (4.19) but with a smoother forcing term. Much work remains to be done in that direction.

Acknowledgements

This work was partially supported by the US AFOSR grant # FA 9550-12-10138.

REFERENCES

AGUI, J. H., BRIASSULIS, G. & ANDREOPOULOS, Y. 2005 Studies of interactions of propagating shock wave with decaying grid turbulence: velocity and vorticity fields. *J. Fluid Mech.* **524**, 143–195.

BATES, J. W. 2012 On the theory of shock wave driven by a corrugated piston in a non-ideal fluid. *J. Fluid Mech.* **691**, 146–164.

BRISCOE, M. G. & KOVITZ, A. A. 1968 Experimental and theoretical study of the stability of plane shock waves reflected normally from perturbed flat walls. *J. Fluid Mech.* **31** (3), 529–546.

CLAVIN, P. 2002*a* Instabilities and nonlinear patterns of overdriven detonations in gases. In *Nonlinear PDE's in Condensed Matter and Reactive Flows* (ed. H. Berestycki & Y. Pomeau), pp. 49–97. Kluwer Academic.

CLAVIN, P. 2002*b* Self-sustained mean streaming motion in diamond patterns of gaseous detonation. *Intl J. Bifurcation Chaos* **12** (11), 2535–2546.

CLAVIN, P & DENET, B. 2002 Diamond patterns in the cellular front of an overdriven detonation. *Phys. Rev. Lett.* **88** (4)044502–1–4.

CLAVIN, P. & WILLIAMS, F. A. 2012 Analytical studies of the dynamics of gaseous detonations. *Phil. Trans. R. Soc* A **370**, 597–624.

D'YAKOV, S. P. 1954 The stabiliy of shockwaves: investigation of the problem of stability of shock waves in arbritary media. *Zh. Eksp. Teor. Fiz.* **27**, 288.

ELLZEY, J. L., HENNEKE, M. R., PICONE, J. M. & ORAN, E. S. 1995 The interaction of a shock with a vortex: Shock distortion and the production of acoustic waves. *Phys. Fluids* **7** (1), 172–184.

GUICHARD, L., VERVICH, L. & DOMINGO, P. 1995 Two-dimensional weak shock–vortex interaction in a mixing zone. *AIAA J.* **33** (10), 1797–1802.

HOWE, M. S. 2003 *Theory of Vortex Sound*. Cambridge University Press.

INOUE, O. 2000 Propagation of sound generated by weak shock–vortex interaction. *Phys. Fluids* **12** (5), 1258–1261.

INOUE, O. & HATTORY, Y. 1999 Sound generation by shock–vortex interactions. *J. Fluid. Mech.* **380**, 81–116.

KONTOROVICH, V. M. 1957 Concerning the stability of shock waves. *Zh. Eksp. Teor. Fiz.* **33**, 1525.

LAPWORTH, K. C. 1959 An experimental investigation of the stability of planar shock waves. *J. Fluid Mech.* **6**, 469–480.

LARSSON, J & LELE, S. K. 2009 Direct numerical simulation of canonical shock/turbulence interaction. *Phys. Fluids* **21**, 126101–1–12.

LELE, S. K. & LARSSON, J. 2009 Shock–turbulence interaction: what we know and what we can learn from peta-scale simulations. *J. Phys.: Conf. Ser.* **180**, 012032.

HUETE RUIZ DE LIRA, C. 2012 Interaction of planar shock waves with non uniforme flows. PhD thesis, Universidad Nacional De Education A Distancia (UNED).

MAJDA, A. & ROSALES, R. 1983 A theory for spontaneous mach stem formation in reacting fronts, I The basic perturbation analysis. *SIAM J. Appl. Maths* **43** (6), 1310–1334.

RIBNER, S. S. 1985 Cylindrical sound wave generated by shock–vortex interaction. *AIAA J.* **23** (11), 1708–1715.

SHCHELKIN, K. I. & TROSHIN, YA. K. 1965 *Gasdynamics of combustion*. Mono Book Corp.

STREHLOW, R. A. 1979 *Fundamentals of Combustion*. Kreiger.

VAN-MOORHEM, K. & GEORGE, A. R. 1975 On the stability of plane shock. *J. Fluid Mech.* **68** (1), 97–108.

WHITHAM, G. B. 1957 A new approach to problem of shock dynamics. Part I two-dimensional problem. *J. Fluid Mech.* **2** (02), 145–171.

WOUCHUK, J. G. & HUETE RUIZ DE LIRA, C. 2009 Analytical linear theory of planar shock wave with isotropic turbulent flow field. *Phys. Rev.* E **79**, 06315–1–35.

ZHANG, S., ZHANG, Y-T. & SHU, C-W. 2005 Multistage interaction of a shock wave and a strong vortex. *Phys. Fluids* **17** (116101), 1–13.